

Dispenser Printed Flexible Rectenna for Dual-ISM Band High-Efficiency Supercapacitor Charging

Mahmoud Wagih, *Graduate Student Member, IEEE*, Alex S. Weddell, *Member, IEEE*,
and Steve Beeby, *Senior Member, IEEE*

School of Electronics and Computer Science, University of Southampton, Southampton, United Kingdom
{mahmlg15, asw, spb}@ecs.soton.ac.uk

Abstract—This paper presents a dual-band sub-1 GHz rectenna for near and far-field powering of Internet of Things (IoT) nodes. The rectifier is based on a coplanar waveguide (CPW) voltage doubler with inductive matching, achieving over 80% power conversion efficiency (PCE) at 10 dBm and 915 MHz. The rectifier is designed to directly charge a 6.8 mF supercapacitor with no DC power management circuitry or load tracking, achieving the highest reported average charging efficiency of 47.2% and 33.3%, at 433 and 915 MHz respectively. From 6 dBm input power, a 1.5-2.8 mA dummy load can be RF-powered with over 30% duty-cycle at 915 MHz. A dual-band single-layer antenna is designed and fabricated using dispenser printing on a flexible polyimide substrate. The antenna maintains over 2.1 dBi gain at 915 MHz with omnidirectional patterns, while occupying under 10×10 cm. The integrated rectenna is evaluated in two real-world applications: energy harvesting from a 915 MHz transmitter showing a 49% wireless charging efficiency for a $7.4 \mu\text{W}/\text{cm}^2$ incident power density; and ambient energy harvesting generating 47 mJ in 5 seconds at 3 to 5 cm from a handheld two-way radio.

Index Terms—Antenna, rectifier, rectenna, supercapacitor, wireless power transmission

I. INTRODUCTION

Wireless power transmission (WPT) in the ultra high frequency (UHF) license-free bands is increasingly seen as a method to power battery-less Internet of Things (IoT) devices [1]. Simple and low-cost rectennas, from UHF to mmWave bands [2], enable more IoT devices to benefit from WPT and ambient radio frequency energy harvesting (RFEH). Compared to ambient RFEH from sources such as GSM or Wi-Fi networks, WPT is more predictable and can deliver power directly to the target device without wasting power omnidirectionally [3]. To reduce the active power transmission time and to enable the wireless nodes to store energy for use when required, an energy storage device (e.g. supercapacitor) is essential to store the rectenna's DC output [3], [4].

A variety of rectennas have been evaluated in conjunction with supercapacitors and batteries [4]–[7]. In [5], a flexible film battery was charged using a spiral rectenna array with 11.6% charging efficiency. A battery-less sensor node was presented in [7] based on a multi-stage voltage multiplier with up to 25% efficiency at 1.2 m. A flexible e-textile rectenna was proposed and integrated with a textile supercapacitor

with up to 37% wireless charging efficiency [4]. Nevertheless, both implementations required complex power management circuitry with over 20 lumped components, adding to the cost and complexity of the system and restricting the rectenna to double/multi-layer printed circuit boards (PCBs) [4].

Realizing rectennas using additive manufacturing has attracted significant interest due to the potential for reducing the rectenna's cost [8], and for enabling rectennas on a variety of substrates. 2.4 GHz [9], sub-1 GHz [10], [11], and millimeter-wave [2], [12] rectennas have been realized using direct-write inkjet and dispenser printing. In [11], where the printed rectenna was used to power a sensor node, the DC power management circuitry, owing to its high-complexity, was integrated on a rigid PCB housing multiple lumped components. Therefore, for printed rectennas to become truly unobtrusive, direct integration with energy storage, with no intermediate DC power management interface, is crucial [4].

In this paper, a direct-written flexible rectenna is proposed for sub-1 GHz dual-ISM band applications, and demonstrated directly charging a 6.8 mF supercapacitor with the highest reported end-to-end average charging efficiency. In Section II, the design and evaluation of a dual-band compact ($0.018\lambda_0$) printed coplanar waveguide (CPW) monopole is presented in Section II-A. The rectifier, achieving a state-of-the-art 80% peak-PCE, is presented in Section III-A. In Section III-B, the rectifier is first studied with the supercapacitor as a load, showing the highest reported RF-charging efficiency of 47.2%. In section III-C, the wireless rectenna is charged from a $7.4 \mu\text{W}/\text{cm}^2$ incident power density at 1.8 m from a 915 MHz source, showing the highest reported wireless charging efficiency of 49%, when operating in the near-field of a 446 MHz two-way radio.

II. DUAL-BAND PRINTED RECTENNA DESIGN

In order to be able to harvest power across both the 915 and 433 MHz license-free sub-1 GHz bands, a dual-band or a broadband antenna is required. However, the long wavelength ($\lambda_{433\text{MHz}}=69$ cm) implies that a broadband antenna will be too large to fit in a compact IoT system. Therefore, antenna miniaturization is of paramount importance. The proposed antenna is based on dual-radiative elements, with folded radiators, to resonate around 433 and 915 MHz. While achieving a 50Ω input impedance is not a design objective in a

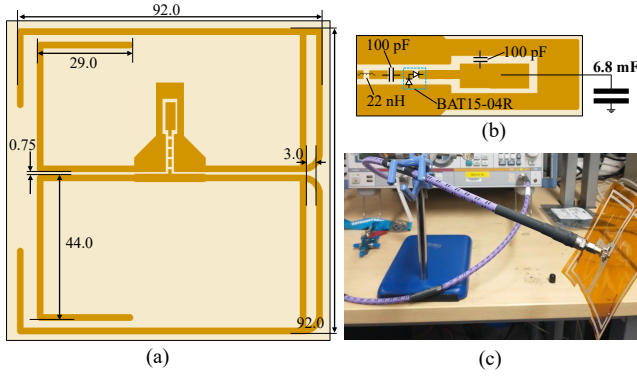


Fig. 1. Layout and photograph of the proposed rectenna: (a) antenna layout and dimensions in mm; (b) layout of the CPW rectifier; (c) photograph of the proposed antenna connected to the VNA for S_{11} measurements.

rectenna, designing the antenna and the rectifier with a 50Ω nominal impedance allows simpler rectifier characterization using standard lab instruments, without the need for wireless testing. The layout and dimensions of the proposed antenna are shown in Fig. 1-a.

The antenna was simulated in CST Microwave Studio and measured experimentally using a Rohde and Schwarz ZVB4 vector network analyzer (VNA), as shown in Fig. 1-c. The antenna was fabricated using direct-write dispenser printing using a Voltera V-One printer and flexible silver ink, using the process detailed in [13] and [10]. The antenna was printed on a flexible $75 \mu\text{m}$ polyimide (Kapton) substrate with $\epsilon_r=3.4$ and $\tan\delta=0.02$. Fig. 2 shows the simulated and measured S_{11} of the antenna, where it can be observed that the antenna resonates around 400 MHz and 900 MHz. At 433 MHz, the antenna's simulated gain is -3.6 dBi with an omnidirectional 3D pattern, owing to its highly miniaturized physical area ($A=0.018\times\lambda_0$). At 915 MHz, the antenna's simulated gain is 3.15 dBi . The antenna's gain at 915 MHz was experimentally measured with respect to a standard 2.1 dBi wire dipole and was found to be above 2 dBi .

III. RECTIFIER DESIGN AND CHARACTERIZATION

The proposed rectifier is based on an inductor-matched voltage doubler, shown in Fig. 1-b. It was previously shown that inductive matching, combined with a miniaturized layout to maintain a high $\Re\{Z_{in}\}$, can achieve a high PCE even on a lossy substrate or conductors [14]. The chosen diode is the Infineon BAT15-04R reverse-pair Schottky diode, the diode was chosen based on its forward voltage (under 300 mV) and its relatively high breakdown voltage of 4 V , enabling high-PCE at a wider input power range than low-breakdown diodes such as the SMS7630. The rectifier was simulated based on its layout, shown in Fig. 1-b, using harmonic balance (HB) simulation in Keysight ADS. The matching inductor value (22 nH) was determined based on the HB simulation to achieve resonance below 1 GHz . The fabricated rectifier prototype was characterized for both a standard resistive load, and by directly connecting a supercapacitor to the rectifier's output.

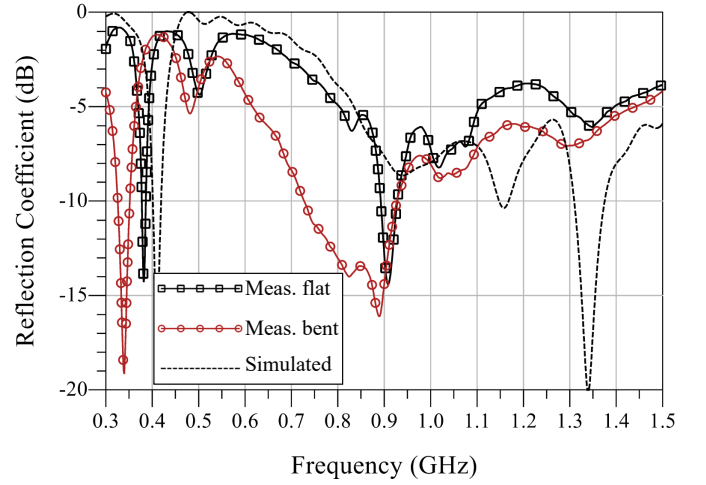


Fig. 2. Simulated and measured reflection coefficient (S_{11}) of the proposed sub-1 GHz antenna.

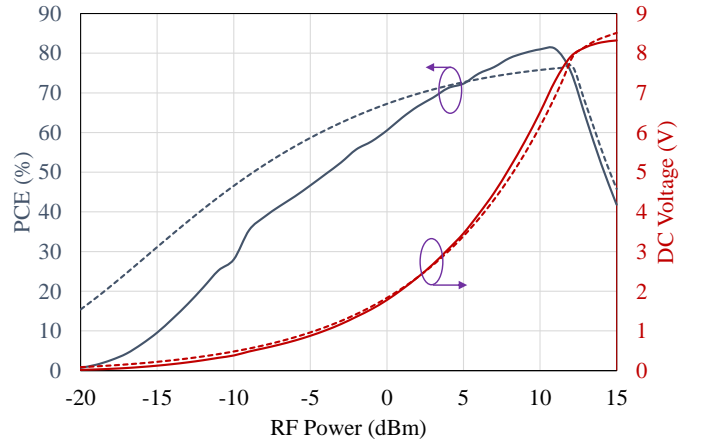


Fig. 3. Simulated and measured DC output and PCE of the voltage doubler rectifier across a $5 \text{ k}\Omega$ load at 915 MHz .

A. Resistive-Loaded Rectifier Characterization

The rectifier was first characterized for a fixed resistive load. The VNA, set to transmit in continuous wave (CW) mode was used to feed the rectifier's coaxial input. A load sweep was carried out, at 0 and 10 dBm RF input, and an optimal load impedance range between 4 and $5 \text{ k}\Omega$ was identified. The input RF power was then swept from -20 to 15 dBm . Fig. 3 shows the measured and HB-simulated DC output of the rectifier and its PCE across an optimal $5 \text{ k}\Omega$ load.

Fig. 3 shows that the rectifier maintains at least 50% PCE above 0 dBm , with a DC voltage output above 3.3 V from 5 dBm input power. Therefore, directly connecting the rectifier to a supercapacitor is expected to charge the energy storage device to a DC potential suitable for powering low-power systems in a short period, owing to the rectifier's relatively low optimal load impedance of $5 \text{ k}\Omega$. Furthermore, the higher DC voltage output exceeding 6 V at 10 dBm implies that a supercapacitor will be charged rapidly to 3.3 V at such high RF input power levels.

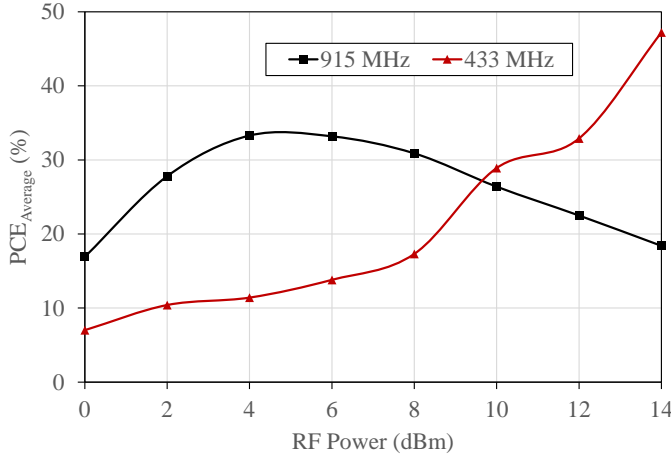


Fig. 4. Measured average RF-charging efficiency of the 6.8 mF supercapacitor at 433 and 915 MHz.

B. Supercapacitor-Loaded Rectifier Characterization

The rectifier's DC output was directly connected to a supercapacitor to characterize its performance while charging an energy storage device. The supercapacitor is a commercially-available AVX BestCap 6.8 mF ultra-low equivalent series resistance (ESR) supercapacitor, rated for up to 15 V DC. The capacitor was chosen based on its small capacitance (resulting in a fast charging time), low profile, and low ESR.

The RF input power to the rectifier was varied and the DC voltage across the capacitor was measured using an oscilloscope. For a capacitive-loaded rectifier, the average charging PCE can be calculated using

$$\text{PCE}_{\text{Average}} = \frac{CV^2}{2} \times \frac{1}{t} \times \frac{1}{P_{\text{RF}}}, \quad (1)$$

where C is the 6.8 mF capacitance, V is the measured DC potential, t is the charging period, and P_{RF} is the input power level [14].

A power sweep was performed using the VNA from 0 to 14 dBm. As previously observed in Fig 3, the rectifier produces over 3.3 V from under 4 dBm input. Therefore, the supercapacitor is charged until a DC voltage of 3.3 V is reached, or until the voltage approaches saturation ($4 \times \tau$) for low P_{RF} levels. Fig. 4 shows the measured charging $\text{PCE}_{\text{Average}}$ at 433 and 915 MHz, where it can be observed that the rectifier achieves at least 10% average charging PCE. In [14], it was previously shown that for a single-series rectifier the average charging PCE is approximately 66% lower than the peak optimal load PCE. Nevertheless, the peak average PCE of the proposed rectifier is only 58% lower than its optimal load PCE, showing its suitability for directly charging a supercapacitor.

To emulate an active IoT low-power node, a dummy 1.2 k Ω load, translating to 1.5-2.8 mA current draw was connected to the supercapacitor. Fig. 5 shows the voltage across the load and the supercapacitor at 433 and 915 MHz, for 6 and 10 dBm RF inputs. In both cases, it can be observed that over a 30%

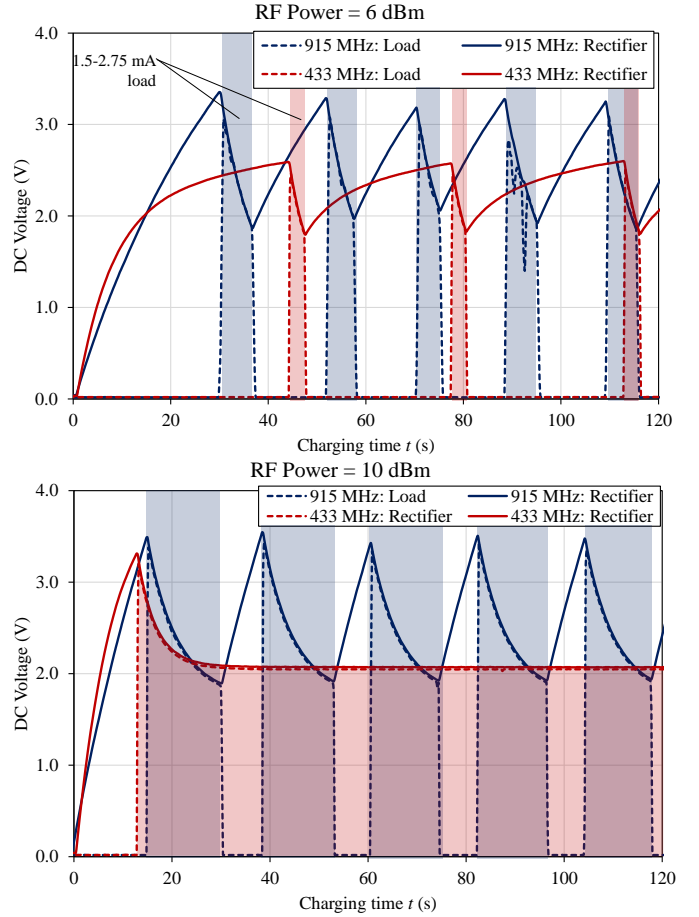


Fig. 5. Measured DC voltage across the RF-charged supercapacitor and load at 915 and 433 MHz; shaded regions indicate the load's active time.

duty cycle can be maintained at 915 MHz from 6 dBm. For a 10 dBm input, the 433 MHz signal is able to sustain the load in continuous operation, above the 1.8 V lower voltage limit.

C. Rectenna Wireless Charging

The rectenna was characterized wirelessly in two use-cases: receiving power from a 3 W (34.77 dBm) 915 MHz license-free source in the far-field at $d=1.8$ m, and harvesting ambient emissions from a handheld 446 MHz two-way radio in close proximity with the rectenna. The inset in Fig 6 shows photographs of both test setups.

The DC output of the rectenna was directly connected to the 6.8 mF supercapacitor and monitored using an oscilloscope. In addition, a 100 k Ω load, translating to approximately 10 μ A DC current draw, was connected as an additional load, emulating the effects of an idle low-power sensor node. Fig 6 shows the measured DC voltage across the supercapacitor for both setups.

From Fig 6-a, it can be observed that the proposed rectenna harvests 36.8 mJ (3.29 V) in 62 seconds. Using (1), an average wireless charging efficiency of 49% is calculated. P_{RF} is assumed to be 1 dBm based on the calculated incident power density $S=7.4 \mu\text{W}/\text{cm}^2$ and a receiving antenna gain

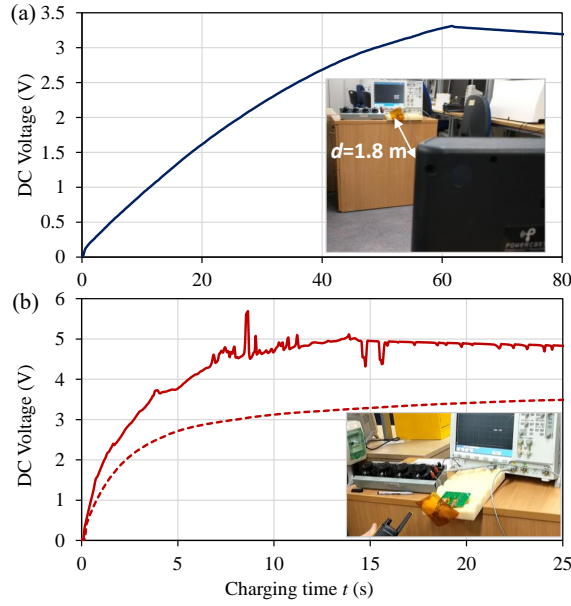


Fig. 6. DC voltage across the supercapacitor during wireless charging from: (a) a Powercast transmitter; (b) two-way radio.

TABLE I
COMPARISON WITH RECENT RECTENNAS CHARGING ENERGY STORAGE

	This work	[5]	[7]	[6]
Freq (MHz)	915; 433	915	915	868
P_{RF} range	0 to 15 dBm	>0 dBm	-4 to 10 dBm	-20 to -5 dBm
Peak PCE	81%	NA	75%	51%
Charging PCE	49%; 47%	11.6%	25%	2%

of 2.1 dBi. By using the gain of a typical $\lambda/2$ dipole, the antenna effect as well as the rectification losses are factored in the PCE, enabling holistic evaluation of the rectenna [10].

In Fig 6-b (solid line), it can be observed that in approximately 5 seconds in very close proximity (3-5 cm) from a 446 MHz handheld radio, the rectenna harvests 47.6 mJ. Furthermore, when the handheld radio-rectenna clearance is increased to 7-10 cm (dashed line), the rectenna still charges the supercapacitor to 3 V in 8 seconds, demonstrating its suitability for both near and far-field RFEH.

The proposed rectenna is compared to recent rectennas directly charging a capacitor in Table I. The rectifier, both when connected to a capacitive or a resistive load, achieves the highest PCE. In addition, the average charging PCE is the highest compared to electrolytic and supercapacitors as well as batteries, while being measured up to 1.8 m from the source. Finally, the antenna's compact size and low complexity show the suitability of the proposed rectenna for printed IoT applications.

IV. CONCLUSION

In this paper, a high-efficiency dual-band sub-1 GHz flexible printed rectenna was proposed for directly charging energy

storage devices. The proposed rectenna achieves the highest reported average RF-charging PCE of 47.2% and 33.3%, at 433 MHz and 915 MHz. The rectenna is highly miniaturized ($0.018\lambda_0$) and is demonstrated in two far and near-field applications. The measured wireless charging efficiency of 49% demonstrates that the proposed rectenna represents a significant improvement over state-of-the-art RFEH systems with energy storage. Finally, this work shows that flexible and additively-manufactured RFEH can be realized with no intermediate DC power management, achieving an unmatched average charging PCE.

REFERENCES

- [1] H. J. Visser and R. J. M. Vullers, "RF Energy Harvesting and Transport for Wireless Sensor Network Applications: Principles and Requirements," *Proc. IEEE*, vol. 101, 6, pp. 1410 – 1423, 2013.
- [2] M. Wagih, A. S. Weddell, and S. Beeby, "Millimeter-Wave Power Harvesting: A Review," *IEEE Open Journal of Antennas and Propagation*, vol. 1, pp. 560 – 578, 2020.
- [3] A. Okba, A. Takacs, and H. Aubert, "Compact rectennas for ultra-low-power wireless transmission applications," *IEEE Trans. Microw. Theory Techn.*, vol. 67, 5, pp. 1697 – 1707, 2019.
- [4] M. Wagih, N. Hillier, S. Yong, A. S. Weddell, and S. Beeby, "RF-Powered Wearable Energy Harvesting and Storage Module based on E-Textile Coplanar Waveguide Rectenna and Supercapacitor," *IEEE Open Journal of Antennas and Propagation*, (In Press).
- [5] W. Zhao, K. Choi, S. Bauman, Z. Dilli, T. Salter, and M. Peckerar, "A radio-frequency energy harvesting scheme for use in low-power ad hoc distributed networks," *IEEE Trans. Circuits And Systems*, vol. 59 no. 9, pp. 573 – 577, 2012.
- [6] A. Okba, D. Henry, A. Takacs, and H. Aubert, "Autonomous RFID Sensor Node Using a Single ISM Band for Both Wireless Power Transfer and Data Communication," *Sensors*, vol. 19 (15), p. 3330, 2019.
- [7] P. Li, Z. Long, and Z. Yang, "RF Energy Harvesting for Battery-Less and Maintenance-Free Condition Monitoring of Railway Tracks," *IEEE Internet of Things Journal*, vol. Early Access, p. DOI: 10.1109/IJOT.2020.3023475, 2020.
- [8] S. A. Nauroze, J. G. Hester, B. K. Tehrani, W. Su, J. Bito, R. Bahr, J. Kimionis, and M. M. Tentzeris, "Additively Manufactured RF Components and Modules: Toward Empowering the Birth of Cost-Efficient Dense and Ubiquitous IoT Implementations," *Proc. IEEE*, vol. 105, no. 4, pp. 702 – 722, 2017.
- [9] A. Eid, J. Hester, J. Costantine, Y. Tawk, A. H. Ramadan, and M. M. Tentzeris, "A Compact Source-Load Agnostic Flexible Rectenna Topology for IoT Devices," *IEEE Trans. Antennas Propag.*, vol. Early Access, pp. 1 – 1, 2019.
- [10] M. Wagih, A. S. Weddell, and S. Beeby, "Meshed High-Impedance Matching Network-Free Rectenna Optimized for Additive Manufacturing," *IEEE Open Journal of Antennas and Propagation*, vol. 1, pp. 615 – 626, 2020.
- [11] J. Bito, J. G. Hester, and M. M. Tentzeris, "Ambient RF Energy Harvesting From a Two-Way Talk Radio for Flexible Wearable Wireless Sensor Devices Utilizing Inkjet Printing Technologies," *IEEE Trans. Microw. Theory Techn.*, vol. 63, 12, pp. 4533–4543, 2015.
- [12] T.-H. Lin, S. N. Daskalakis, A. Georgiadis, and M. M. Tentzeris, "Achieving fully autonomous system-on-package designs: An embedded-on-package 5g energy harvester within 3d printed multilayer flexible packaging structures," in *2019 IEEE MTT-S International Microwave Symposium (IMS)*, 2019.
- [13] M. Wagih, "Direct-Write Dispenser Printing for Rapid Antenna Prototyping on Thin Flexible Substrates," in *2020 European Conference on Antennas and Propagation (EuCAP)*, 2020.
- [14] M. Wagih, A. S. Weddell, and S. Beeby, "Omnidirectional Dual-Polarized Low-Profile Textile Rectenna with over 50% Efficiency for Sub- $\mu\text{W}/\text{cm}^2$ Wearable Power Harvesting," *IEEE Trans. Antennas Propag.*, vol. Early Access, 2020.